Static spike autosolitons in the Gray-Scott model

Static spike autosolitons in the Gray–Scott model

C B Muratov† and V V Osipov‡

† Department of Mathematical Sciences, New Jersey Institute of Technology, University Heights, Newark, NJ 07102, USA
‡ CSIC, Laboratorio de Física de Sistemas Pequeños y Nanotecnología, Calle Serrano, 144, 28006, Madrid, Spain

E-mail: `muratov@m.njit.edu` and `osipov@fsp.csic.es`

Abstract.   We construct asymptotically the solutions to a classical reaction–diffusion system (the Gray–Scott model of an autocatalytic reaction) in the form of static spike autosolitons (self-sustained solitary pulses, spots and clots). We show that solutions in the form of static spike autosolitons exist over a wide range of system parameters in one dimension, and in a narrower range of parameters in two and three dimensions. We study the properties of these solutions.

1. Introduction

Self-organization and pattern formation in non-equilibrium systems are among the most fascinating phenomena in nonlinear physics [1–11]. Pattern formation is observed in various physical systems including fluids; gas and electron–hole plasmas; semiconductor, superconductor and gas-discharge structures; some ferroelectric, magnetic and optical media; combustion systems (see, for example, [5, 9–14]), as well as in many chemical and biological systems (see, for example, [1–7, 15]).

Self-organization is often associated with the destabilization of the homogeneous state of the system [1, 2, 5, 10, 11]. At the same time, when the homogeneous state of the system is stable, one can excite large-amplitude patterns, including *autosolitons* (ASs; self-sustained solitary inhomogeneous states) by applying a sufficiently strong localized perturbation [8–11, 16–19]. Autosolitons are elementary objects in open dissipative systems away from equilibrium. They share properties of both solitons and travelling waves (or autowaves, as they are also referred to [2, 6]). They are similar to solitons since they are localized objects whose existence is due to the nonlinearities of the system. On the other hand, from the physical point of view they are essentially different from solitons in that they are *dissipative structures*, that is, they are self-sustained objects which form in strongly dissipative systems as a result of the balance between the dissipation and pumping of energy or matter. This is the reason why, in contrast to solitons, their properties are independent of the initial conditions and are determined primarily by the nonlinearities of the system [8–11]. ASs can be static, pulsating or travelling. As a result of their various instabilities, these simplest localized patterns can spontaneously transform into complex space-filling static or dynamic patterns, including complex pulsating and travelling patterns, or spatio-temporal chaos [8–14, 18–33].

A prototype model used to study pattern formation in non-equilibrium systems is a pair of reaction–diffusion equations of the activator–inhibitor type,

$$\tau_\theta \frac{\partial \theta}{\partial t} = l^2 \Delta \theta - q\,(\theta, \eta, A) \tag{1.1}$$

$$\tau_\eta \frac{\partial \eta}{\partial t} = L^2 \Delta \eta - Q\,(\theta, \eta, A) \tag{1.2}$$

where θ is the activator, η is the inhibitor, τ_θ, l and τ_η, L are the time and length scales of the activator and the inhibitor, respectively; A is the control (bifurcation) parameter; q and Q are certain nonlinear functions representing the activation and the inhibition processes. Examples of these equations for various physical systems are given in [9–13, 25] where the physical meaning of the variables θ and η and the nature of the activation and the inhibition processes are discussed.

The fact that θ is the activator means that for certain parameters the uniform fluctuations of θ will grow when the value of η is fixed. From the mathematical point of view, this is given by the condition [9–11, 18]

$$\frac{\partial q}{\partial \theta} < 0 \tag{1.3}$$

for certain values of θ and η. On the other hand, the fact that η is the inhibitor means that its own fluctuations decay and that it damps the fluctuations of the activator. Mathematically, these conditions are expressed by [9–11, 18]

$$\frac{\partial Q}{\partial \eta} > 0 \qquad \frac{\partial q}{\partial \eta} \frac{\partial Q}{\partial \theta} < 0 \tag{1.4}$$

for all values of θ and η, provided that the derivatives in equation (1.4) do not change sign.

Kerner and Osipov showed [8–11, 16–18, 25] that the properties of patterns and self-organization scenarios in systems described by equations (1.1) and (1.2) are chiefly determined by the parameters $\epsilon \equiv l/L$ and $\alpha \equiv \tau_\theta/\tau_\eta$ and the shape of the nullcline of the equation for the activator, that is, the dependence $\eta(\theta)$ given by the equation $q(\theta, \eta, A) = 0$ for $A = $ constant. They demonstrated that depending on the shape of the activator nullcline the majority of systems can be divided into two fundamentally different classes: N-systems, for which the nullcline is N- or inverted N-shaped and, Λ- or V-systems, for which the nullcline is Λ- or V-shaped, respectively (see figure 1).

Let us emphasize that smallness of ϵ and/or α is a necessary condition for the feasibility of any patterns [9–11]. Indeed, if both the characteristic time and length scales of the variation
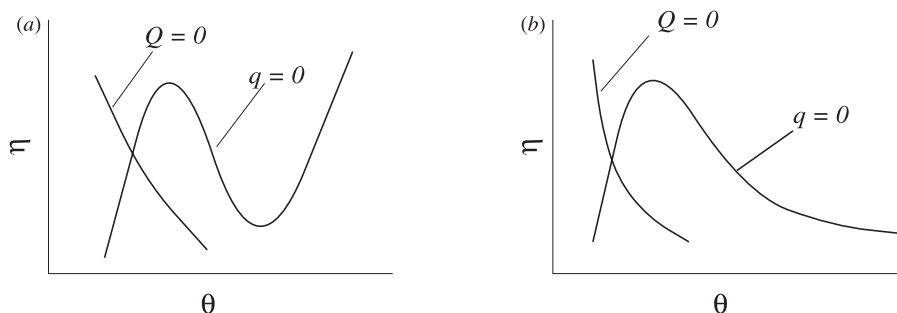

Figure 1. Two qualitatively different types of the nullclines of equations (1.1) and (1.2): (*a*) N-systems and (*b*) Λ-systems.

of the inhibitor were much smaller than those of the activator, the inhibitor would easily damp all the deviations of the activator from the homogeneous steady state, making the formation of any kind of persistent patterns impossible.

Most works devoted to the description of pattern formation on the basis of equations (1.1) and (1.2) deal with N-systems. For these models it was shown [27] that equations (1.1) and (1.2) with $L = 0$ and $\alpha \ll 1$ have solutions in the form of travelling waves (also called autowaves [2, 6], or travelling ASs [8–11]). In [16–19] it was shown that in another limit $\epsilon \ll 1$ equations (1.1) and (1.2) admit solutions in the form of the static patterns including ASs [16–19], see also [9–11]. Furthermore, it was shown that in systems with $\epsilon \ll 1$ and $\alpha \ll 1$ one can excite static, pulsating, and travelling patterns [8–11, 18, 25, 28–33]. In N-systems with $\epsilon \ll 1$ static ASs and other patterns are essentially domains of high and low values of the activator separated by interfaces (walls) in which θ varies sharply by a quantity of the order of one over a distance of the order of l. The characteristic size $\mathcal{L}_s$ of these domain patterns lies in the range $l \ll \mathcal{L}_s \lesssim L$ [9–11, 17–21].

At the same time, there are many physical, chemical and biological systems for which the activator nullcline is Λ- or V-shaped (figure 1(*b*)) [1, 9–12, 16, 25, 34, 35]. Kerner and Osipov showed qualitatively that in Λ-systems the so-called spike ASs and more complex spike patterns can be excited [9, 11, 16, 36, 37]. They analysed the static spike ASs and strata in the Brusselator, the Gierer–Meinhardt model and the electron–hole plasma [16, 36]. They found that when $\epsilon \ll 1$, the one-dimensional static spike AS can have a small size of the order of l and a huge amplitude which goes to infinity as $\epsilon \to 0$. Dubitskii, Kerner and Osipov formulated the asymptotic procedure for finding the stationary solutions in Λ-systems for sufficiently small ϵ [11, 36]. Recently, we showed that in another limiting case $\alpha \ll 1$ and $\epsilon \gg 1$, one can excite the one-dimensional travelling spike AS, which also has small size and whose amplitude goes to infinity as $\alpha \to 0$ [38]. Osipov and Severtsev studied one-dimensional static spike ASs in the linearized version of the Gray–Scott model [39] and in the Gierer–Meinhardt model in higher dimensions [40]. One can see that the properties of the spike patterns forming in Λ-systems differ fundamentally from those of the domain patterns forming in N-systems. At the same time, spike patterns including spike ASs are observed experimentally in nerve tissue [41], chemical reactions [5, 42], electron–hole plasma [43], gas-discharge structures [44], as well as numerically in the simulations of the Brusselator, the Gierer–Meinhardt and the Gray–Scott models [1, 26, 34, 45].

In this paper we present an asymptotic study of the static spike ASs in the Gray–Scott model of an autocatalytic chemical reaction. We chose the Gray–Scott model because it has the advantage having relatively simple nonlinearities, which in many cases allow us to obtain explicit analytic results. Also, because of this one can expect a certain degree of universality of pattern formation exhibited by it. We will study the static spike ASs in the Gray–Scott model with $\epsilon \ll 1$ in one, two and three dimensions.

The outline of our paper is as follows. In section 2 we introduce the model we will study, in section 3 we construct the solutions in the form of the one-dimensional static spike AS; in section 4 we construct the solution in the form of the three-dimensional radially symmetric static spike AS; in section 5 we do that for the two-dimensional radially symmetric static spike AS; in section 6 we discuss recent works of other authors on the Gray–Scott model and compare their results with ours, and in section 7 we draw conclusions.

2. The model

The Gray–Scott model describes the kinetics of a simple autocatalytic reaction in an unstirred flow reactor. The reactor is a narrow space between two porous walls. Substance Y whose

concentration is kept fixed outside of the reactor is supplied through the walls into the reactor with rate k_0 and the products of the reaction are removed from the reactor with the same rate. Inside the reactor Y undergoes the reaction involving an intermediate species X:

$$2X + Y \xrightarrow{k_1} 3X \tag{2.1}$$

$$X \xrightarrow{k_2} \text{inert.} \tag{2.2}$$

The first reaction is a cubic autocatalytic reaction resulting in self-production of species X; therefore, X is the activator species. On the other hand, the production of X is controlled by species Y, so Y is the inhibitor species. The equations of chemical kinetics which describe the spatiotemporal variations of the concentrations of X and Y in the reactor and take into account the supply and removal of the substances through the porous walls take the following form [35]:

$$\frac{\partial X}{\partial t} = -(k_0 + k_2)X + k_1 X^2 Y + D_X \Delta X \tag{2.3}$$

$$\frac{\partial Y}{\partial t} = k_0(Y_0 - Y) - k_1 X^2 Y + D_Y \Delta Y \tag{2.4}$$

where now X and Y are the concentrations of the activator and the inhibitor species, respectively, Y_0 is the concentration of Y in the reservoir, Δ is the two-dimensional Laplacian, and D_X and D_Y are the diffusion coefficients of X and Y.

In order to be able to understand various pattern formation phenomena in a system of this kind, it is crucial to introduce the variables and the time and length scales that truly represent the physical processes acting in the system. The first and the most important is the choice of the characteristic time scales. These are primarily dictated by the time constants of the dissipation processes. For Y this is the supply and removal at a rate of k_0, whereas for X this is the removal from the system and the decay via the second reaction with the total rate $k_0 + k_2$. The natural way to introduce the dimensionless inhibitor concentration is to scale it with Y_0. Since we want to fix the time scale of variation of the inhibitor (with the fixed activator), we will rescale X in such a way that the reaction term in equation (2.4) will generate the same time scale as the dissipative term. This leads to the following positive dimensionless quantities:

$$\theta = X/X_0 \qquad \eta = Y/Y_0 \qquad X_0 = \left(\frac{k_0}{k_1}\right)^{1/2}. \tag{2.5}$$

The characteristic time and length scales for these quantities are

$$\tau_\theta = (k_0 + k_2)^{-1} \qquad \tau_\eta = k_0^{-1} \tag{2.6}$$

$$l = (D_X \tau_\theta)^{1/2} \qquad L = \left(D_Y \tau_\eta\right)^{1/2}. \tag{2.7}$$

If we now write equations (2.3) and (2.4) in the dimensionless form, we will arrive at the following set of equations:

$$\tau_\theta \frac{\partial \theta}{\partial t} = l^2 \Delta \theta + A\theta^2 \eta - \theta \tag{2.8}$$

$$\tau_\eta \frac{\partial \eta}{\partial t} = L^2 \Delta \eta - \theta^2 \eta + 1 - \eta \tag{2.9}$$

where we have introduced a dimensionless parameter

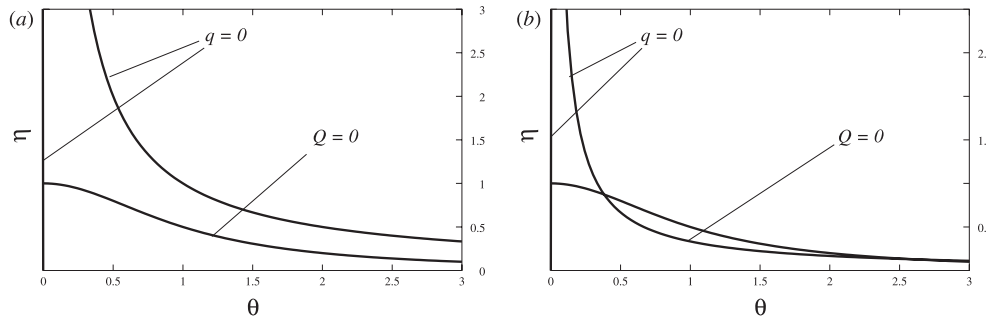$$A = \frac{Y_0 k_0^{1/2} k_1^{1/2}}{(k_0 + k_2)}. \tag{2.10}$$

Figure 2. The nullclines of equations (2.8) and (2.9) for (*a*) $A = 1$ and (*b*) $A = 3$.

One can see from equations (2.8) and (2.9) that τ_θ and τ_η are, in fact, the characteristic time scales, and l and L the characteristic length scales of variation of small deviations of θ and η from the stationary homogeneous state $\theta = \theta_h$ and $\eta = \eta_h$:

$$\theta_h = 0 \qquad \eta_h = 1. \tag{2.11}$$

Thus, the system is characterized by only three dimensionless parameters: $\alpha \equiv \tau_\theta/\tau_\eta$, $\epsilon \equiv l/L$ and A. As can be seen from equation (2.8), the parameter A is the dimensionless strength of the activation process, that is, it describes the degree of deviation of the system from thermal equilibrium. With all of this, equations (2.8) and (2.9) are reduced to the form of equations (1.1) and (1.2). Note that the system given by equations (2.8) and (2.9) is indeed a system of the activator–inhibitor type: the condition in equation (1.3) is satisfied for $\theta > \frac{1}{2A\eta}$, and the conditions in equation (1.4) are satisfied with $\partial q/\partial\eta < 0$ and $\partial Q/\partial\theta > 0$ for all $\theta > 0$ and $\eta > 0$.

The nullclines of equations (2.8) and (2.9) are shown in figure 2. From this figure one can see that the nullcline of the equation for the activator has a degenerate Λ-form. It consists of two separate branches: $\theta = 0$ and $1/A\eta$. Note that adding an extra small constant term on the right-hand side of equation (2.8) (which physically would correspond to some finite concentration of substance X in the reservoir), one can remove this degeneracy of the nullcline and make the nullcline truly Λ-shaped.

One can easily check that for $0 < A < 2$ there is only one stationary homogeneous state given by equation (2.11), whereas for $A > 2$ two extra stationary homogeneous states exist

$$\theta_{h2,3} = \frac{A \mp \sqrt{A^2 - 4}}{2} \qquad \eta_{h2,3} = \frac{A \pm \sqrt{A^2 - 4}}{2A}. \tag{2.12}$$

The stability analysis of these homogeneous states shows that for $\epsilon \ll 1$ or $\alpha \ll 1$ the homogeneous state $\theta = \theta_{h2}$, $\eta = \eta_{h2}$ is always unstable. For $\epsilon \ll 1$ the homogeneous state $\theta = \theta_{h3}$, $\eta = \eta_{h3}$ is unstable with respect to the Turing instability if $A < 0.41\epsilon^{-1}$. For $\alpha \ll 1$ it is unstable with respect to the homogeneous oscillations (Hopf bifurcation) if $0.41\alpha^{-1/2} < A < \alpha^{-1/2}$, or it is an unstable node if $A < 0.41\alpha^{-1/2}$. On the other hand, the homogeneous state $\theta = \theta_h$, $\eta = \eta_h$ is stable for all values of the system's parameters. The latter is simple to understand: in order for the reaction to begin there has to be at least some amount of activator put in at the start. Equivalently, the fact that the homogeneous state in equation (2.11) is stable for all values of the parameter A (for an arbitrary deviation from thermal equilibrium) is the consequence of the degeneracy of the nullcline of equation (2.8). Thus, self-organization associated with the Turing instability of the homogeneous state $\theta_h = 0$ and $\eta_h = 1$ is not realized in the Gray–Scott model. In such a stable homogeneous system

any inhomogeneous pattern, including the ASs, can only be excited by a sufficiently strong localized stimulus. In turn, self-organization will occur as a result of the instabilities of the large-amplitude patterns already present in the system.

In the case of $\epsilon \ll 1$ and $\alpha \ll 1$ the largest length scale in the system is L and the longest time scale is τ_η, so it is natural to scale length and time with L and τ_η, respectively. In these units equations (2.8) and (2.9) take the following form:

$$\alpha \frac{\partial \theta}{\partial t} = \epsilon^2 \Delta \theta + A\theta^2 \eta - \theta \tag{2.13}$$

$$\frac{\partial \eta}{\partial t} = \Delta \eta - \theta^2 \eta + 1 - \eta. \tag{2.14}$$

We will assume that the problem is defined on the sufficiently large domain with zero flux boundary conditions. Note that the kinetic model used to arrive at equations (2.13) and (2.14) imposes a restriction $\alpha \leqslant 1$ (see equation (2.6)). Also, in the derivation we assumed that the system is essentially two dimensional. For the sake of generality, in the following we will allow α to take arbitrary values and will work with an arbitrary dimensional Gray–Scott model.

3. One-dimensional static spike autosoliton

Let us now study the simplest possible stationary pattern in the Gray–Scott model—the static spike AS. According to the general qualitative theory, these ASs form in Λ-systems when $\epsilon \ll 1$ [9–11, 16]. We begin with the analysis of the one-dimensional static spike AS. In the Gray–Scott model it is described by the following equations:

$$\epsilon^2 \frac{d^2\theta}{dx^2} + A\theta^2\eta - \theta = 0 \tag{3.1}$$

$$\frac{d^2\eta}{dx^2} - \theta^2\eta + 1 - \eta = 0. \tag{3.2}$$

Since $\epsilon \ll 1$, there is a strong separation of length scales in the AS [9–11, 16]. One can separate the spike region where the distribution of θ varies on a length scale of ϵ, and the periphery of the AS where η decays to the homogeneous state $\eta_h = 1$ on a length scale of the order of unity. One can use this separation of length scales to construct a singular perturbation theory which describes the distributions in the form of the static one-dimensional spike AS [36]. However, before we do that, it is instructive to use a more qualitative approach which will give us an idea concerning the scaling of the main parameters of the AS and its qualitative shape. As will be seen below, this approach works when $\epsilon^{1/2} \lesssim A \ll 1$.

3.1. Case $A \sim \epsilon^{1/2}$: autosoliton collapse

According to this approach [9–11, 16], one assumes that the value of η inside the spike (on a length scale of ϵ) is close to a constant value η_s. This is a reasonable assumption as long as $\eta \gg \epsilon$ in the spike since the characteristic length scale of variation of η is 1. Then, equation (3.1) with $\eta = \eta_s$ can be solved exactly. Its solution has the form

$$\theta(x) = \theta_m \cosh^{-2}\left(\frac{x}{2\epsilon}\right) \qquad \text{with} \quad \theta_m = \frac{3}{2A\eta_s}. \tag{3.3}$$

On the other hand, the distribution of θ given by equation (3.3) acts in equation (3.2) as a δ-function, so away from the spike the distribution of η is given by

$$\eta(x) = 1 - \frac{3\epsilon}{\eta_s A^2} e^{-|x|}. \tag{3.4}$$

Now, matching this solution for $\eta(x)$ with the condition that $\eta(0) = \eta_s$, we obtain the following expressions:

$$\theta_m = \frac{3A}{A_b^2} \left[1 \pm \sqrt{1 - \frac{A_b^2}{A^2}} \right] \qquad \eta_s = \frac{A_b^2}{2A^2} \left[1 \pm \sqrt{1 - \frac{A_b^2}{A^2}} \right]^{-1} \tag{3.5}$$

where

$$A_b = \sqrt{12\epsilon}. \tag{3.6}$$

Note that equation (3.6) was obtained independently in [46] by applying Melnikov analysis to equations (3.1) and (3.2). Similar results for the simplified version of the Gray–Scott model were obtained in [39].

From equation (3.5) one can see that at $A < A_b$ the solution in the form of the spike AS does not exist. When $A > A_b$ there are two solutions: the one corresponding to the plus sign has a larger amplitude and the one corresponding to the minus sign has smaller amplitude. As was shown by Kerner and Osipov, the solutions that have a smaller amplitude are always unstable [9–11], so the only interesting solution corresponds to the plus sign in equation (3.5). This solution is precisely the static spike AS. The numerical simulations of equations (2.13) and (2.14) show that if the value of A is lowered, at $A = A_b$ a stable one-dimensional static spike AS collapses into the homogeneous state [47].

Let us look more closely at the parameters of the static spike AS and the conditions of validity of the approximations made in the preceding paragraphs. As can be seen from equations (3.3) and (3.4), the distribution of the activator indeed has a form of the spike whose characteristic width is of the order of ϵ, and the distribution of the inhibitor varies on the much larger length scale of the order of unity. Also, according to equation (3.5), the amplitude of the spike at A close to A_b is of the order of $\epsilon^{-1/2} \gg 1$ (and can, in fact, have huge values as ϵ becomes smaller) and grows as the value of A increases. At $A \sim 1$ the amplitude $\theta_m \sim \epsilon^{-1}$. These features differ fundamentally, the ASs forming in Λ-systems from the ASs in N-systems.

Recall that in the derivation we have neglected the variation of the inhibitor inside the spike. Since the characteristic length of variation of η is of the order of unity, this means that the value of $\eta = \eta_s$ in the centre of the AS must be much greater than ϵ. According to equation (3.5), this is indeed the case as long as $A \ll 1$, so the solution obtained above is a good approximation to the actual solution in this case. Also, in this case one can easily calculate the distribution of η in the spike. To do this, we note that, according to equation (3.5), for $A \ll 1$ we have $\theta^2 \eta \gg 1$ in the spike, so the last two terms in equation (3.2) can be neglected. Since the variation of η in the spike is much smaller compared with η_s, we can also put $\eta = \eta_s$ there. Then, substituting θ from equation (3.3) into this equation, after simple integration we obtain an expression for η in the spike region

$$\eta(x) = \eta_s + \frac{4\epsilon^2 \theta_m^2 \eta_s}{3} \left(2 \ln \cosh \frac{x}{2\epsilon} + \frac{1}{2} \tanh^2 \frac{x}{2\epsilon} \right). \tag{3.7}$$

3.2. Case $A \sim 1$: local breakdown

On the other hand, according to equations (3.5), when $A \sim 1$, we have

$$\theta_{\max} \sim \epsilon^{-1} \qquad \eta_{\min} \sim \epsilon \tag{3.8}$$

and the approximation used by us ceases to be valid. However, it is clear that qualitatively the character of the solution should not change even for these values of A. Therefore, we can still assume that the spike of the AS has a width of the order of ϵ and that the values of the activator and the inhibitor scale in the same way as those in equation (3.8). With all this in mind, we are now able to introduce singular perturbation expansion and separate the 'sharp' distributions (inner solutions) that vary on the length scale of ϵ and the 'smooth' distributions (outer solutions) that vary on the length scale of the order of unity.

At distances much greater than ϵ away from the spike (in the outer region) the value of θ is exponentially zero. This follows from the fact that in the region of the smooth distributions θ and η are related locally through the equation $q(\theta, \eta) = 0$ and therefore must lie on the stable branch of the nullcline of the equation for the activator [9–11]. In the case of the Gray–Scott model this gives an especially simple relation: $\theta = 0$. So, the equation for the smooth distributions becomes

$$\frac{\mathrm{d}^2\eta}{\mathrm{d}x^2} + 1 - \eta = 0 \tag{3.9}$$

with the boundary condition in the spike $\eta(0) = 0$ (to order ϵ) and $\eta = \eta_h$ at infinity. This immediately gives us the smooth distribution of η

$$\eta(x) = 1 - \mathrm{e}^{-|x|}. \tag{3.10}$$

Let us scale the activator and the inhibitor according to equation (3.8) and introduce the stretched variable ξ:

$$\tilde{\theta} = \epsilon\theta \qquad \tilde{\eta} = \epsilon^{-1}\eta \qquad \xi = \frac{x}{\epsilon}. \tag{3.11}$$

Using these variables, after a little algebra we can write equations (3.1) and (3.2) as

$$\tilde{\theta}_{\xi\xi} + A\tilde{\theta}^2\tilde{\eta} - \tilde{\theta} = 0 \tag{3.12}$$

$$\tilde{\eta}_{\xi\xi} = A^{-1}(\tilde{\theta} - \tilde{\theta}_{\xi\xi}) \tag{3.13}$$

where we kept only the leading terms. In this equation $\tilde{\theta}_{\xi\xi}$ denotes the second derivative with respect to ξ. Thus, the solution of equations (3.12) and (3.13) properly matched with the smooth distribution, given by equation (3.10), will give the sharp distributions of the activator and the inhibitor in the spike.

The matching of the sharp and the smooth distributions is performed by noting that, according to equation (3.11), to order ϵ we have $\eta = 0$ and $\eta_x \sim 1$ for $\epsilon \ll |x| \ll 1$. Therefore, it is the derivative of η obtained from the sharp distribution at $|\xi| \gg 1$ that must coincide with that of the smooth distribution for $|x| \ll 1$. This condition is obtained by imposing the boundary condition $\tilde{\eta}_\xi(\pm\infty) = \pm 1$ in equation (3.13) (see equation (3.10)). One can obtain an integral representation of this boundary condition by integrating equation (3.13) over ξ. Let us introduce the variables

$$\bar{\theta} = \frac{\tilde{\theta}}{A} \qquad \bar{\eta} = \tilde{\eta} + \frac{\tilde{\theta}}{A}. \tag{3.14}$$

Then, this integral condition takes the form

$$\int_{-\infty}^{+\infty} \bar{\theta} \, \mathrm{d}\xi = 2|\lambda|^{-1/2} \tag{3.15}$$

where λ is a constant that should be equal to -1 (the reason for introducing this coefficient will be explained in the following paragraph). In terms of the new variables equation (3.13) becomes especially simple,

$$\bar{\eta}_{\xi\xi} = |\lambda|\bar{\theta} \tag{3.16}$$

where λ is the same constant. Note that equation (3.16) has an obvious symmetry which allows us to add an arbitrary constant to $\bar{\eta}$, so we can replace $\bar{\eta} \to \bar{\eta} + \bar{\eta}_s$, where $\bar{\eta}$ satisfies the condition $\bar{\eta}(0) = \bar{\eta}_\xi(0) = 0$ and thus is uniquely determined by $\bar{\theta}$, and $\bar{\eta}_s$ is an arbitrary constant.

To analyse equations (3.12) and (3.13), it is convenient to rewrite them as a nonlinear eigenvalue problem

$$\left[-\frac{\mathrm{d}^2}{\mathrm{d}\xi^2} + V(\xi) \right] \bar{\theta} = \lambda\bar{\theta} \tag{3.17}$$

$$V(\xi) = -A^2\bar{\theta}(\bar{\eta}_s + \bar{\eta} - \bar{\theta}) \tag{3.18}$$

where $\bar{\eta}$ is, in turn, related to $\bar{\theta}$ via equation (3.16). Then, since $\bar{\theta}$ is positive for all ξ and therefore has no nodes, the solution in the form of the static spike AS will correspond to the lowest bound state of the operator in equation (3.17) with $\lambda = -1$. The latter is achieved by adjusting the value of $\bar{\eta}_s$.

The nonlinear eigenvalue problem given by equations (3.17) and (3.18) together with equations (3.15) and (3.16) with fixed $\bar{\eta}_s$ can be solved iteratively. Indeed, for a given potential well V there is a unique eigenvalue λ and a unique eigenfunction $\bar{\theta}$ (up to normalization) that correspond to the lowest bound state of the Schrödinger operator in equation (3.17). Equation (3.15) gives a unique normalization for $\bar{\theta}$, which then uniquely determines $\bar{\eta}$ through equation (3.16). Knowing the distributions $\bar{\theta}$ and $\bar{\eta}$, one can then reconstruct the potential V', thus defining an iterative map. It is convenient to think of the solutions of the nonlinear eigenvalue problem as fixed points of this iterative map.

Observe that the nonlinear eigenvalue problem is invariant with respect to the following transformation:

$$\xi \to \frac{\xi}{b} \qquad \lambda \to b^2\lambda \qquad A \to bA \tag{3.19}$$

where b is an arbitrary positive constant. It is clear that if one knows a solution of the nonlinear eigenvalue problem with certain λ, one can obtain a solution of equations (3.12) and (3.13) by simply using the symmetry transformation in equation (3.19) with $b = |\lambda|^{-1/2}$, so there is, in fact, a one-to-one correspondence between the solutions of the nonlinear eigenvalue problem with arbitrary λ and its solution with $\lambda = -1$, which corresponds to the sharp distributions.

Since we are interested in the lowest bound state whose eigenvalue is equal to -1, the characteristic length scale of the variation of $\bar{\theta}$ and, according to equation (3.16), of $\bar{\eta}$ and V as well, is of the order of unity. Equation (3.15) fixes the normalization of $\bar{\theta}$, so we must have $\bar{\theta} \sim 1$. Note that in view of equation (3.16) and the fact that $\bar{\theta} \sim 1$, we must always have $\bar{\eta} \sim 1$.

Let us write the potential V in equations (3.17) and (3.18) as a sum of two parts: $V = V_0 + V_1$, where

$$V_0 = -A^2\bar{\theta}\bar{\eta}_s \qquad V_1 = -A^2\bar{\theta}(\bar{\eta} - \bar{\theta}). \tag{3.20}$$

From the qualitative form of $\tilde{\eta}(\xi)$ (see, for example, equation (3.7)) it is easy to see that the potential V_0 has the form of a simple potential well, while V_1 has the form of a double well (see figure 3).
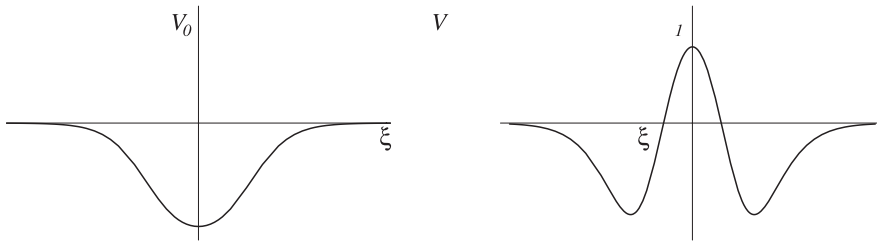
Figure 3. Qualitative form of the potentials V_0 and V_1 from equations (3.20).
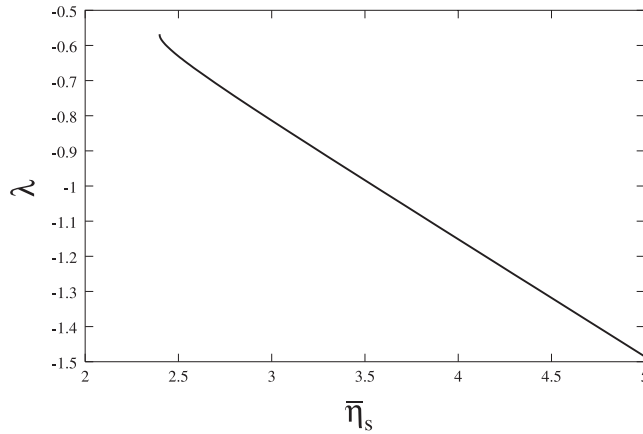

Figure 4. Dependence $\lambda(\bar{\eta}_s)$ for the one-dimensional static AS. Results of the numerical solution of the nonlinear eigenvalue problem with $A = 1$.

In order for the operator in equation (3.17) to have the lowest bound state with $\lambda = -1$ the potential V must have a depth of the order of unity. When $A \ll 1$, the function $\tilde{\eta}(\xi)$ must be chosen in such a way that it compensates for the small factor of A in equation (3.20). However, since $\bar{\eta} \sim 1$, this can only be achieved by choosing $\bar{\eta}_s \sim A^{-2} \gg 1$. This means that we will have $V_0 \gg V_1$. If one neglects V_1 compared with V_0, one can solve the nonlinear eigenvalue problem exactly. This solution will be

$$\bar{\theta}(\xi) = \tfrac{1}{2} \cosh^{-2} \left(\tfrac{1}{2} \xi \right) \qquad \bar{\eta}_s = \frac{3}{A^2}. \tag{3.21}$$

The potential V_1 can then be treated as a perturbation which will give corrections to $\bar{\theta}$ and $\bar{\eta}$, so one should not expect any qualitative changes in the behaviour of the solution for $A \lesssim 1$.

In the other limiting case $A \gg 1$ the nonlinear eigenvalue problem will not have solutions with $\lambda = -1$. Indeed, in this case the potential V is always deep with a depth $\gtrsim A^2$ regardless of the choice of $\bar{\eta}_s$, so the lowest eigenvalue of the operator in equation (3.17) will be $|\lambda| \sim A^2 \gg 1$ (assuming that V varies on a length scale of the order of unity). This means that the solution in the form of the static spike AS exists only when $A \lesssim 1$. Note that this result was obtained independently in [48] by the method of topological shooting.

The numerical solution of the nonlinear eigenvalue problem shows that for $A = 1$ and arbitrary λ (recall that the solutions for all other values of A can be obtained using the symmetry transformation given by equation (3.19)) there exists a unique stable solution for all $\bar{\eta}_s$ greater than some critical value $\bar{\eta}_s^*$ (see figure 4). This can be explained in the following way. For large
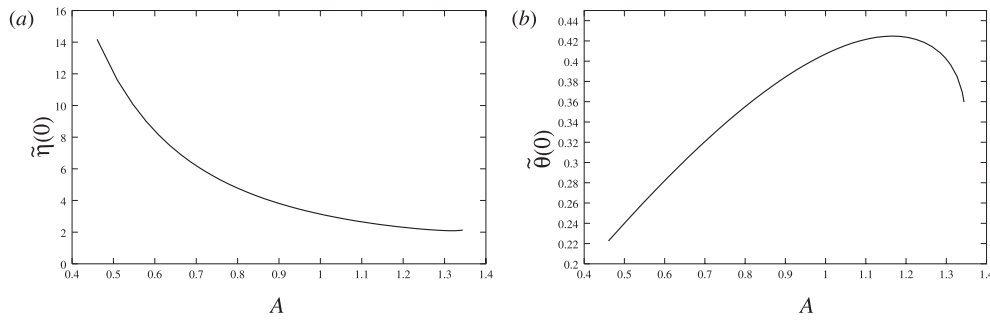
Figure 5. The values of (*a*) $\tilde{\eta}(0)$ and (*b*) $\tilde{\theta}(0)$ as functions of *A* for the one-dimensional AS obtained from the numerical solution of equations (3.12) and (3.13).

enough values of $\bar{\eta}_s$ the potential V_0, which can always produce a localized state, dominates in the total potential V. As the value of $\bar{\eta}_s$ decreases, the effect of the potential V_1 becomes more and more pronounced, so V gradually transforms from a single-well to a double-well potential. This means that with decreasing $\bar{\eta}_s$ the function $\bar{\theta}$ will tend to localize in the minima of V_1 instead of the minimum of V_0 (see figure 3). On the other hand, the localization of $\bar{\theta}$ in the minima of V_1 will in turn increase V_1, since the latter is self-consistently determined by $\bar{\theta}$ (see equation (3.16)). If one constructs the solution of the nonlinear eigenvalue problem iteratively, for small enough values of $\bar{\eta}_s$ one will find that at each step of the iterations the potential V is such that at the next step the distribution of $\bar{\theta}$ will become localized further and further away from the origin. On the other hand, it is easy to show that there is no solution of the nonlinear eigenvalue problem in the form of a pair of spikes some distance $L \gtrsim 1$ apart. Suppose that we have a solution in the form of two spikes centred at $\xi = \pm L/2$, with $L \gg 1$. Let us multiply equation (3.17) by $\bar{\theta}_\xi$ and integrate it over positive ξ. As a result, using the fact that for $L \gg 1$ with exponential accuracy $\bar{\theta}(0) = 0$, we obtain the relation $A^2 \int_0^\infty \bar{\theta}^3 \bar{\eta}_\xi \, d\xi = 0$. This relation, however, cannot be satisfied since the function $\bar{\eta}_\xi$ is positive definite for all positive ξ, so the solution of the assumed form does not exist. So, for $\bar{\eta}_s < \bar{\eta}_s^*$ the iterative procedure will not converge and at $\bar{\eta}_s = \bar{\eta}_s^*$ the solution of the nonlinear eigenvalue problem abruptly disappears.

From figure 4 one can see that λ is a monotonically decreasing function of $\bar{\eta}_s$, with its maximum attained at $\bar{\eta}_s = \bar{\eta}_s^* \simeq 2.40$ for $A = 1$ (see figure 4). According to equation (3.19), we have $|\lambda_{\max}| = |\lambda(\bar{\eta}_s^*)| = \text{constant}/A^2$. Therefore, at some $A = A_d \sim 1$ we will have $\lambda_{\max} = -1$, so that for $A > A_d$ there will be no solutions corresponding to the one-dimensional static spike AS. Thus, at $A = A_d$ there is a bifurcation of the static spike AS which results in the local breakdown and leads to its splitting and self-replication [47].

The numerical solution of equations (3.12) and (3.13) together with equation (3.15) confirm our conclusions concerning the behaviour of the sharp distributions as the value of A is varied. Figure 5 shows the dependences of the values of $\tilde{\theta}$ and $\tilde{\eta}$ at $\xi = 0$ on A obtained from the numerical solution of equations (3.12) and (3.13). From this figure one can see that the solution indeed disappears at $A = A_d$ with the value of A_d found to be $A_d = 1.35$. Figure 6 shows the distributions of $\tilde{\theta}$ and $\tilde{\eta}$ in the spike obtained from the numerical solution of equations (3.12) and (3.13) for a particular value of A. It also shows the entire solution obtained by matching the sharp and smooth distributions for the particular values of A and ϵ. Note that the distributions given by equations (3.21) give a very good approximation to the actual solution whenever A is not in the immediate vicinity of A_d (for example, at $A < 0.8$ these distributions give solutions with an accuracy of better than 10%).
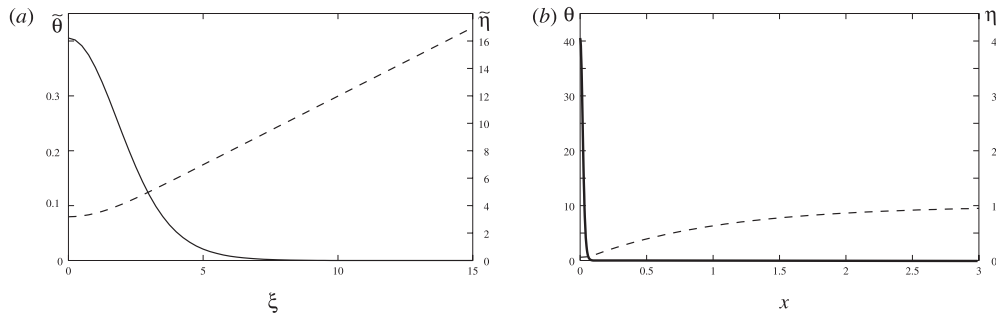
Figure 6. (*a*) Sharp distributions $\tilde{\theta}(\xi)$ (full curve) and $\tilde{\eta}(\xi)$ (broken curve) in a one-dimensional static AS, obtained from the numerical solution of equations (3.12) and (3.13) with $A = 1$; (*b*) The full solution for θ (full curve) and η (broken curve) at $A = 1$ and $\epsilon = 0.01$.

3.3. Case $\epsilon^{1/2} \ll A \ll 1$

Let us now consider the intermediate case $\epsilon^{1/2} \ll A \ll 1$. In this case the results of sections 3.1 and 3.2 both predict for θ and η in the spike

$$\theta(x) = \frac{A}{2\epsilon} \cosh^{-2} \left(\frac{x}{2\epsilon} \right) \qquad \eta_s = \frac{3\epsilon}{A^2} \tag{3.22}$$

and the correction to η to be given by equation (3.7) with $4\epsilon^2\theta_m^2\eta_s/3 = \epsilon$ (see equations (3.5) for $A \gg \epsilon^{1/2}$). Note that equations (3.22) were independently obtained in [46].

Observe that the procedure presented in section 3.2 is valid with accuracy ϵ when $A \sim 1$. For these values of A it is justified to assume in the matching condition that with this accuracy $\eta(0) = 0$. As the value of A decreases, the actual value of $\eta(0) \sim \epsilon/A^2$ grows, so the accuracy of the above-mentioned approximation decreases, and at $A \sim \epsilon^{1/2} \sim A_b$ this approximation becomes invalid. On the other hand, in the procedure discussed in section 3.1 the matching condition uses the true value of $\eta(0) \sim 1$ for $A \sim A_b$, but neglects the variation of η in the spike. The latter gives the corrections of the order of A^2 to the solution given by equation (3.3), which are of the order of ϵ when $A \sim A_b$ and grow as A increases. For $A \sim \epsilon^{1/4}$ both of these procedures give the same solutions with an accuracy of $\epsilon^{1/2}$, so, in fact, for $\epsilon \ll 1$ one can construct the solution in the form of the static spike AS asymptotically for all values of A. When $A \lesssim \epsilon^{1/4}$, one should use the procedure described in section 3.1 and when $A \gtrsim \epsilon^{1/4}$ one should use that of section 3.2.

Above we presented the ways to construct asymptotically the solution in the form of the one-dimensional static spike AS. As such, these procedures should be good only for sufficiently small values of $\epsilon \ll 1$. According to the analysis above, this AS exists in a wide range $A_b < A < A_d$ with $A_b \sim \epsilon^{1/2} \ll 1$ and $A_d \sim 1$. This implies that in order for the whole asymptotic procedure to be in quantitative agreement with the actual solution we must have $A_b \ll A_d$. In view of equation (3.6), this will be the case when $\epsilon \lesssim 0.03$.

4. Three-dimensional radially symmetric static spike autosoliton

Let us now study higher-dimensional static spike ASs. These are radially symmetric spikes of large amplitude and size of the order of ϵ [9–11]. As we will show below, in the Gray–Scott model the properties of the solutions in the form of the higher-dimensional radially symmetric spike ASs turn out to be different from those of the static spike AS in one dimension.

Let us consider a three-dimensional AS first. The distributions of θ and η in the form of the AS will be determined by equations (2.13) and (2.14) in which the time derivatives are set to zero and only the radially symmetric part of the Laplacian is retained, with the spike centred at zero. When $\epsilon \ll 1$, one can once again use singular perturbation theory and separate the sharp distributions (inner solutions) in the spike from the smooth distributions (outer solutions) away from the spike.

As in the case of the one-dimensional AS, away from the spike the activator and the inhibitor become decoupled, so that $\theta = 0$ there and the smooth distribution of η is given by

$$\eta(r) = 1 - \frac{a e^{-r}}{r} \tag{4.1}$$

where r is the radial coordinate and a is a certain constant (see equation (2.14)). The constant a is determined by the strength of the δ-function-like source term at $r = 0$. Integrating equations (2.13) and (2.14) over the spike region, we obtain that

$$a = \frac{1}{A} \int_0^\infty r^2 \theta(r)\, dr \tag{4.2}$$

where the integration was extended to the whole space since $\theta = 0$ away from the spike. One can see an important difference between equation (4.1) and equation (3.10) for the one-dimensional AS: in the case of the three-dimensional AS the derivative of η with respect to r in the smooth distribution becomes singular at $r = 0$. This means that the scaling of θ and η in the spike will be different from that of the one-dimensional AS. Indeed, for $r \sim \epsilon$ the value of η must be positive, so we must have $a \sim \epsilon$. According to equation (4.2), this implies that in the spike $\theta \sim A\epsilon^{-2}$. Also, from equation (4.1) one can see that near the spike η varies by values of the order of unity on the length scale of ϵ. Since we must have $A\theta^2\eta \sim \theta$ in equation (2.13) in the spike region to have a solution, the scaling for the variables and the parameter A will be the following:

$$\theta_{\max} \sim \epsilon^{-1} \qquad \eta_{\min} \sim 1 \qquad A \sim \epsilon. \tag{4.3}$$

Introducing the scaled quantities and the stretched variable

$$\tilde{\theta} = \epsilon\theta \qquad \tilde{\eta} = \eta \qquad \tilde{A} = \epsilon^{-1}A \qquad \xi = \frac{r}{\epsilon} \tag{4.4}$$

and retaining only the leading terms in equations (2.13) and (2.14), we can write the equations describing the sharp distributions (inner solutions) of the activator and the inhibitor in the spike as

$$\frac{d^2\tilde{\theta}}{d\xi^2} + \frac{d-1}{\xi}\frac{d\tilde{\theta}}{d\xi} + \tilde{A}\tilde{\theta}^2\tilde{\eta} - \tilde{\theta} = 0 \tag{4.5}$$

$$\frac{d^2\tilde{\eta}}{d\xi^2} + \frac{d-1}{\xi}\frac{d\tilde{\eta}}{d\xi} - \tilde{\theta}^2\tilde{\eta} = 0 \tag{4.6}$$

with $d = 3$ (for generality we set an arbitrary dimensionality of space d in equations (4.5) and (4.6)). The boundary conditions are neutral at $\xi = 0$, and zero for $\tilde{\theta}$ at infinity. The precise boundary condition for $\tilde{\eta}$ at infinity which ensures proper matching between the sharp and smooth distributions has to be specified. To do this, we note that, according to equation (4.1), to order ϵ we have $\eta = 1$ at $r \gg \epsilon$ (or $\xi \gg 1$). This means that the boundary condition for $\tilde{\eta}$ in equation (4.6) must be taken to be $\tilde{\eta}(\infty) = 1$.

It is convenient to perform the following change of variables:

$$\tilde{\theta} = \frac{\tilde{A}\bar{\theta}}{\xi} \qquad \tilde{\eta} = \bar{\eta}_s + \frac{\bar{\eta} - \bar{\theta}}{\xi} \tag{4.7}$$

where we define $\bar\eta(0) = \bar\eta_\xi(0) = 0$. Obviously, $\bar\eta_s$ must satisfy $0 < \bar\eta_s < 1$. In these variables, we can write equation (4.5) in the form of the nonlinear eigenvalue problem

$$\left[-\frac{\mathrm{d}^2}{\mathrm{d}\xi^2} + V(\xi) \right] \bar\theta = \lambda\bar\theta \tag{4.8}$$

$$V(\xi) = -\frac{\tilde{A}^2\bar\theta}{\xi}\left(\bar\eta_s + \frac{\bar\eta - \bar\theta}{\xi} \right) \tag{4.9}$$

and equation (4.6) as

$$\bar\eta_{\xi\xi} = |\lambda|\bar\theta \tag{4.10}$$

where we must have $\lambda = -1$ for the sharp distributions. The problem now has a one-dimensional form similar to that in section 3, but is defined for $\xi > 0$, with zero boundary condition for $\bar\theta$ at $\xi = 0$. As in the one-dimensional case, the solution that corresponds to the AS must be the lowest bound state and have $\lambda = -1$. The latter is achieved by adjusting the value of $\bar\eta_s$. Also, according to the definition of $\bar\eta$, the matching condition $\tilde\eta(\infty) = 1$ corresponds to the boundary condition $\bar\eta_\xi(\infty) = 1 - \bar\eta_s$ for equation (4.10). Integrating equation (4.10) with $\lambda = -1$ over ξ, we transform it into an integral condition

$$\int_0^\infty \bar\theta \, \mathrm{d}\xi = 1 - \bar\eta_s. \tag{4.11}$$

This condition fixes the normalization of $\bar\theta$.

It is possible to show that the nonlinear eigenvalue problem possesses a continuous symmetry generated by

$$\frac{\mathrm{d}\xi}{\mathrm{d}b} = -\xi$$

$$\frac{\mathrm{d}\lambda}{\mathrm{d}b} = 2\lambda$$

$$\frac{\mathrm{d}\bar\eta_s}{\mathrm{d}b} = 2\bar\eta_s(1 - \bar\eta_s)$$

$$\frac{\mathrm{d}\bar\theta}{\mathrm{d}b} = \bar\theta(1 - 2\bar\eta_s) \tag{4.12}$$

$$\frac{\mathrm{d}\bar\eta}{\mathrm{d}b} = \bar\eta(1 - 2\bar\eta_s)$$

$$\frac{\mathrm{d}\tilde{A}}{\mathrm{d}b} = -\tilde{A}(1 - 2\bar\eta_s).$$

From these equations one can see that if there is a solution of the nonlinear eigenvalue problem with certain $\bar\eta_s$, λ and A, there is also a solution with

$$\lambda' = \lambda\frac{\bar\eta_s'(1 - \bar\eta_s)}{\bar\eta_s(1 - \bar\eta_s')} \qquad \tilde{A}' = \tilde{A}\left[\frac{\bar\eta_s(1 - \bar\eta_s)}{\bar\eta_s'(1 - \bar\eta_s')} \right]^{1/2} \tag{4.13}$$

with $\bar\eta_s'$ arbitrary. Since $\lambda'(\bar\eta_s')$ is a monotonic function of $\bar\eta_s'$ that goes from 0 to infinity as $\bar\eta_s'$ changes from 0 to 1, for any $\bar\eta_s$ it is always possible to choose a unique value of $\bar\eta_s'$ for which $\lambda' = -1$. So, as in the one-dimensional case, there is a one-to-one correspondence between the solutions of the nonlinear eigenvalue problem with arbitrary λ and the sharp distributions.
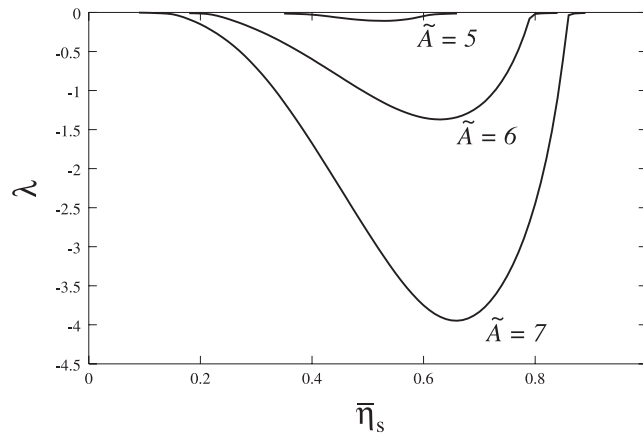
Figure 7. Dependence $\lambda(\bar{\eta}_s)$ for the three-dimensional radially symmetric AS. Results of the numerical solution of the nonlinear eigenvalue problem for different values of $\tilde{A}$.

The potential V can be written as a sum of two parts: $V = V_0 + V_1$, where

$$V_0 = -\frac{\tilde{A}^2 \bar{\theta} \bar{\eta}_s}{\xi} \qquad V_1 = -\frac{\tilde{A}^2 \bar{\theta}(\bar{\eta} - \bar{\theta})}{\xi^2}. \tag{4.14}$$

The qualitative form of these potentials for sufficiently small values of $\tilde{A}$ coincides with that shown in figure 3 for $\xi > 0$. According to equations (4.10) and (4.11), at these values of $\tilde{A}$ we have the following estimates for V_0 and V_1 when $\bar{\eta}_s$ is close to either 1 or 0:

$$V_0 \sim -\bar{\eta}_s(1 - \bar{\eta}_s) \qquad V_1 \sim -(1 - \bar{\eta}_s)^2. \tag{4.15}$$

In writing these estimates, we used the fact that the characteristic length scale of the variation of $\bar{\theta}$ and $\bar{\eta}$ is 1.

4.1. Case $A \sim \epsilon$: autosoliton collapse

For $\tilde{A} \sim 1$, one can analyse the solutions of the nonlinear eigenvalue problem in the following way. First of all, for sufficiently small values of $\tilde{A}$ the potential V will be so shallow that there will be no bound states in the eigenvalue problem at all. When the value of $\tilde{A}$ is increased, at some $\tilde{A} = \tilde{A}_0$ the potential V will become capable of localizing a state at $\bar{\eta}_s \sim \frac{1}{2}$ (see equation (4.15)). When the value of $\tilde{A}$ is increased further, the minimum value of $\lambda = \lambda_{\min}$ will decrease, so that at some $\tilde{A} = \tilde{A}_b$ we will have $\lambda_{\min} = -1$ (see figure 7 in which the numerical solution of the nonlinear eigenvalue problem for several values of $\tilde{A}$ is shown). For $\tilde{A} > \tilde{A}_b$ we will have $\lambda_{\min} < -1$, so there will be two values of $\bar{\eta}_s$ at which $\lambda = -1$ (figure 7). Therefore, the solutions of the nonlinear eigenvalue problem with these values of $\bar{\eta}_s$ will correspond to the sharp distributions we are looking for. Thus, the solution in the form of the three-dimensional static spike AS exists only for $\tilde{A} > \tilde{A}_b$. From the numerical solution of equations (4.5) and (4.6) we obtain that in this case $\tilde{A}_b = 5.8$.

It is possible to show that the solution corresponding to the largest value of $\bar{\eta}_s$ should be unstable. Indeed, if the value of $\bar{\eta}_s$ is decreased, we will have an increase in V_1 and a decrease in V_0. Since V_1 can localize $\bar{\theta}$ more easily than V_0, a small decrease of $\bar{\eta}_s$ will produce such a deviation of $\bar{\theta}$ that will (through equations (4.10) and (4.14)) further distort the potential V in the same manner. In other words, if we construct an iterative map that takes V, calculates

the solution $\bar\theta$ of the eigenvalue problem, and then generates a new V by solving for $\bar\eta$, it will take us from the unstable solution with greater $\bar\eta_s$ to the stable solution with lower $\bar\eta_s$ if $\bar\eta_s$ is decreased at the start, or to the trivial solution $\tilde\theta = 0$ and $\tilde\eta = 1$, which is obviously stable, if the value of $\bar\eta_s$ is increased. Thus, the solution corresponding to the stable radially symmetric static AS should be unique.

4.2. Case $A \gg \epsilon$: annulus

The numerical solution of equations (4.5) and (4.6) shows that for $\tilde A$ not far from $\tilde A_b$ the distribution of θ in the AS has the form of a spike centred at zero. As the value of $\tilde A$ increases, the shape of the AS changes. To see how the AS behaves as the value of $\tilde A$ is increased, a special treatment of the case $\tilde A \gg 1$ is needed. When $\tilde A$ becomes large, the potential V contains a large factor of $\tilde A$. This factor can be compensated by choosing, for example, $1 - \bar\eta_s \sim \tilde A^{-2} \ll 1$, which will correspond to the unstable solution with larger $\bar\eta_s$. Alternatively, one could have the potential V shifted along ξ, so that it is centred around $\xi = R \gg 1$. In other words, one can look for sharp distributions in the form of an annulus of radius R. In that case the main contribution to V will be given by $V_0 \sim -\tilde A^2/R$ for $\bar\eta_s$ not close to either 0 or 1. Since $\bar\theta$ decays exponentially at large distances from $\xi = R$, for $R \gg 1$, the boundary conditions at $\xi = 0$ become inessential and can be moved to minus infinity. In this case, if one neglects the terms of the order of $1/R$ in the potential, one can solve the nonlinear eigenvalue problem exactly. The solution will be given by

$$\bar\theta = \frac{1 - \bar\eta_s}{4} \cosh^{-2}\left(\frac{\xi - R}{2}\right) \tag{4.16}$$

with

$$R = \frac{A^2 \bar\eta_s (1 - \bar\eta_s)}{6}. \tag{4.17}$$

So far, we have obtained a continuous family of solutions parametrized by $\bar\eta_s$ in the case $\tilde A \gg 1$. This result may seem surprising, since for $\tilde A \sim 1$ we showed that there should be only one stable solution to the nonlinear eigenvalue problem. However, as we will show below, all the solutions found in the preceding paragraph except for a single solution are, in fact, structurally unstable, so the stable solution is indeed unique for $\tilde A \gg 1$.

The reason for the structural instability of the solutions with $R \gg 1$ is that in the limit $R \to \infty$ the problem possesses translational symmetry. As a result, for $R \gg 1$ there is a degenerate mode corresponding to translations of the spike as a whole along ξ. One should therefore study the stability of the solution with respect to that mode.

To analyse the stability of the solutions with $R \gg 1$, we need to calculate the $1/R$ correction to the solution obtained above. Let us write equations (4.5) and (4.6) in a form that is valid to order $1/R$

$$\tilde\theta_{\xi\xi} + c\tilde\theta_\xi + \frac{2\tilde\theta_\xi}{R} + \tilde A\tilde\theta^2\tilde\eta - \tilde\theta = 0 \tag{4.18}$$

$$\tilde\eta_{\xi\xi} - \bar\eta_s\tilde\theta^2 = 0 \tag{4.19}$$

where for the solution sought we must have $c = 0$. We wrote equation (4.18) so that it is reminiscent of an equation describing the solution travelling with constant speed c. In fact, if one solves this problem for c as a function of R coupled to the equation $\mathrm{d}R/\mathrm{d}t = c(R)$ and equation (4.17), one should be able to describe slow variations of the radius of the annulus.

We can use the expression for $\bar{\theta}$ obtained above to calculate the variation of $\tilde{\eta}$ in the spike. Integrating equation (4.19) with $\tilde{\theta}$ from equation (4.16) and using the boundary condition $\tilde{\eta}_\xi(-\infty) = 0$, we obtain

$$\tilde{\eta} = \bar{\eta}_s + \frac{1 - \bar{\eta}_s}{2R} \left(2\ln\cosh\frac{\xi - R}{2} + \frac{1}{2}\tanh^2\frac{\xi - R}{2} + \xi - R \right). \tag{4.20}$$

Substituting this expression for $\tilde{\eta}$ into equation (4.18), multiplying it by $\tilde{\theta}_\xi$, and integrating over ξ, for $\bar{\eta}_s < \frac{1}{2}$ we obtain the following expression for c:

$$c = \frac{1}{\tilde{A}^2} \left[-\frac{2\tilde{A}^2}{R} + \frac{12}{1 - 12R/\tilde{A}^2 - \sqrt{1 - 24R/\tilde{A}^2}} \right]. \tag{4.21}$$

In writing this equation we assumed the relationship between $\bar{\eta}_s$ and R from equation (4.17).

The analysis of equation (4.21) shows that we have $c = 0$ only for $R = R^*$ (and $\bar{\eta}_s = \bar{\eta}_s^*$), where

$$R^* = \tfrac{1}{27}\tilde{A}^2 \qquad \bar{\eta}_s^* = \tfrac{1}{3}. \tag{4.22}$$

Thus, the corrections of the order of $1/R$ destroy the solutions with $R \neq R^*$.

Consider the flow generated by the equation $dR/dt = c(R)$. The behaviour of this flow near the fixed point $R = R^*$ should determine the stability of the solution. According to equation (4.21), we have $c > 0$ for $R < R^*$ and $c < 0$ for $R > R^*$, so the flow is into the fixed point. Therefore, the solution with $R = R^*$ is stable. One can also write an equation similar to equation (4.21) in the case $\bar{\eta}_s > \frac{1}{2}$, which corresponds to another branch of the solutions obtained above. The analysis of this equation shows that for those solutions $c < 0$ for all $\bar{\eta}_s$, so the flow transforms the solution into the trivial solution $\tilde{\theta} = 0$. Thus, the solution that corresponds to the radially symmetric static AS is indeed unique even for $\tilde{A} \gg 1$.

4.3. Comparison of the two cases

From the arguments given above it is clear that when the value of $\tilde{A}$ is increased from $\tilde{A}_b \sim 1$ to $\tilde{A} \gg 1$, the solution in the form of the AS should gradually transform from a spike to an annulus of large radius $R \sim \tilde{A}^2$. This is what we see from the numerical solution of equations (4.5) and (4.6). Figure 8 shows the dependence $\tilde{\eta}(0)$ and $\tilde{\theta}(0)$ as a function of $\tilde{A}$ in the radially symmetric AS obtained from this solution. From this figure one can see that $\tilde{\eta}(0)$
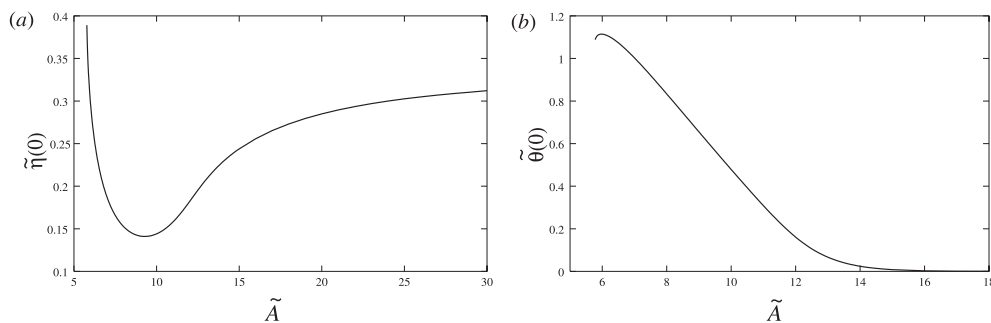

Figure 8. The values of (a) $\tilde{\eta}(0)$ and (b) $\tilde{\theta}(0)$ as functions of $\tilde{A}$ for the three-dimensional radially symmetric AS obtained from the numerical solution of equations (4.5) and (4.6).
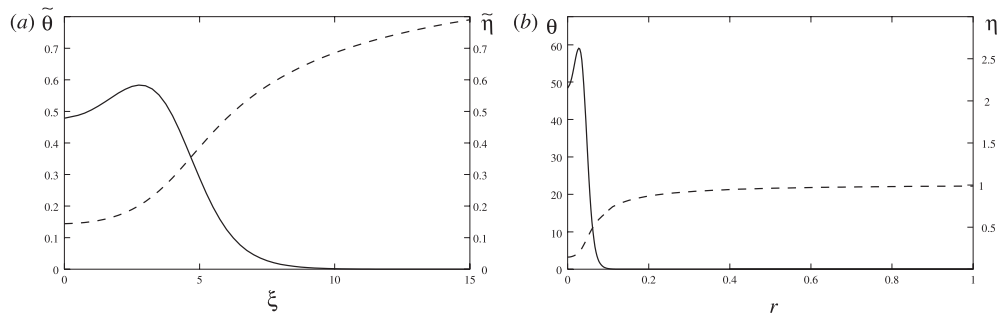
Figure 9. (*a*) Sharp distributions $\tilde{\theta}(\xi)$ (full curve) and $\tilde{\eta}(\xi)$ (broken curve) in a three-dimensional radially symmetric static AS, obtained from the numerical solution of equations (4.5) and (4.6) with $\tilde{A} = 10$; (*b*) construction of the full solution for θ (full curve) and η (broken curve) at $A = 0.1$ and $\epsilon = 0.01$.

indeed approaches $\bar{\eta}_s^* = \frac{1}{3}$ as $\tilde{A}$ increases. The dependence of the radius of the annulus was also found to be in good agreement with equation (4.22) for large values of $\tilde{A}$.

Figure 9 shows the distributions of $\tilde{\theta}$ and $\tilde{\eta}$ in the radially symmetric three-dimensional AS for a particular value of $\tilde{A}$ which is intermediate between the spike and the annulus. This figure also shows the entire solution in the form of an AS obtained by matching the sharp and the smooth distributions for the particular values of A and ϵ.

So far we have studied the situations when $R \gg 1$ but still smaller than the inhibitor length, which in these units is of the order of ϵ^{-1}. When R reaches this value, equations (4.5) and (4.6) will no longer be justified for the description of the distributions of θ and η in the annulus. In the unscaled variables this will happen when $A \sim \epsilon^{1/2} \sim A_b^{(1)}$ (see equation (4.22)), where $A_b^{(1)}$ is the minimum value of A at which the one-dimensional static AS exists (see section 3.1). At these values of A the radially symmetric AS can effectively be considered as a one-dimensional AS, so when A reaches some value $A_d \sim \epsilon^{1/2}$, the solution in the form of an annulus will transform into a quasi-one-dimensional AS of infinite radius. Note, however, that this bifurcation point is essentially different from the bifurcation at $A = A_d$ of the one-dimensional AS (section 3.2) in that it does not involve local breakdown or splitting of the AS.

5. Two-dimensional static spike autosoliton

Let us now turn to the two-dimensional case. The analysis of the two-dimensional radially symmetric static AS turns out to be analogous to that of the three-dimensional AS, so we will not go into much detail here, but will only give the main results.

As in the case of the three-dimensional AS, away from the spike $\theta = 0$, the distribution of η is given by

$$\eta(r) = 1 - aK_0(r) \tag{5.1}$$

where K_0 is the modified Bessel function, r is the radial coordinate and a is a certain constant. The value of a is determined by integrating equations (2.13) and (2.14) with the time derivatives set to zero over the spike region. In two dimensions a is given by

$$a = \frac{1}{A} \int r\theta(r) \, dr. \tag{5.2}$$

According to equation (5.1), when r becomes of the order of ϵ, we have

$$\eta \simeq 1 - a \ln \epsilon^{-1} + a \ln(r/\epsilon). \tag{5.3}$$

In order for η to remain positive, we must have $a \sim 1/\ln \epsilon^{-1}$. Then, on the length scales of ϵ the variation of η in the spike will be of the order of $a \ll 1$. In the same way as in the case of the three-dimensional AS, this results in the following scaling for the main parameters of the AS:

$$\theta_{\max} \sim \epsilon^{-1} \qquad \eta_{\min} \sim \frac{1}{\ln \epsilon^{-1}} \qquad A \sim \epsilon \ln \epsilon^{-1}. \tag{5.4}$$

In the scaled variables

$$\tilde{\theta} = \epsilon\theta \qquad \tilde{\eta} = \eta \ln \epsilon^{-1} \qquad \tilde{A} = \frac{A}{\epsilon \ln \epsilon^{-1}} \qquad \xi = \frac{r}{\epsilon} \tag{5.5}$$

the equations for the sharp distributions in the spike will take the form of equations (4.5) and (4.6) with $d = 2$. Since the variation of η in the spike is of the order of $1/\ln \epsilon^{-1}$, according to equation (5.3) we must have $a = 1/\ln \epsilon^{-1}$ in the limit $\epsilon \to 0$. This gives us the condition for matching the sharp and the smooth distributions. Let us introduce the variables

$$\bar{\theta} = \tilde{A}^{-1}\tilde{\theta} \qquad \bar{\eta} = \tilde{\eta} + \tilde{A}^{-1}\tilde{\theta} - \bar{\eta}_s \tag{5.6}$$

where $\bar{\eta}_s$ is a constant that is chosen so that $\bar{\eta}(0) = 0$. Then, the matching condition can be written in the integral form as

$$\int_0^\infty \bar{\theta}\xi \, d\xi = |\lambda|^{-1} \tag{5.7}$$

where λ is a constant that must be equal to –1. Also, in terms of the new variables the equation for the sharp distribution of $\bar{\eta}$ can be written as

$$\frac{1}{\xi}\frac{d}{d\xi}\left(\xi\frac{d\bar{\eta}}{d\xi}\right) = |\lambda|\bar{\theta} \tag{5.8}$$

with $\bar{\eta}_\xi(0) = 0$.

As with the three-dimensional AS, in two dimensions the problem of finding the sharp distributions can be written as a nonlinear eigenvalue problem

$$-\frac{1}{\xi}\frac{d}{d\xi}\left(\xi\frac{d\bar{\theta}}{d\xi}\right) + V(\xi)\bar{\theta} = \lambda\bar{\theta} \tag{5.9}$$

$$V(\xi) = -\tilde{A}^2\bar{\theta}(\bar{\eta}_s + \bar{\eta} - \bar{\theta}) \tag{5.10}$$

with the potential V that can be separated as $V = V_0 + V_1$, where

$$V_0 = -\tilde{A}^2\bar{\theta}\bar{\eta}_s \qquad V_1 = -\tilde{A}^2\bar{\theta}(\bar{\eta} - \bar{\theta}). \tag{5.11}$$

These potentials have the form shown in figure 3 for $\xi > 0$. The lowest bound state with $\lambda = -1$ will give us the solution we are looking for. This condition is achieved by adjusting the value of $\bar{\eta}_s$. The nonlinear eigenvalue problem is invariant with respect to the transformation given by equation (3.19).

When $\tilde{A} \ll 1$, the potential V acquires a small factor (as in the case of the one-dimensional AS), which can be compensated only by choosing $\bar{\eta}_s \sim \tilde{A}^{-2} \gg 1$. Therefore, the potential V will be dominated by V_0 which can always localize a bound state with $\lambda = -1$. Note, however, that in order for the approximations made to derive the equations for the sharp distributions to remain valid, we must have $\bar{\eta}_s \lesssim \ln \epsilon^{-1}$, so, in fact, this argument is valid only down to
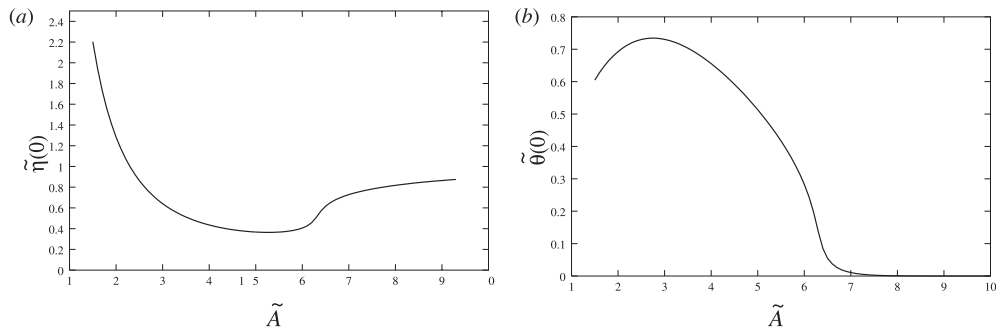
Figure 10. The values of (*a*) $\tilde{\eta}(0)$ and (*b*) $\tilde{\theta}(0)$ as functions of $\tilde{A}$ for the two-dimensional radially symmetric AS obtained from the numerical solution of equations (4.5) and (4.6).
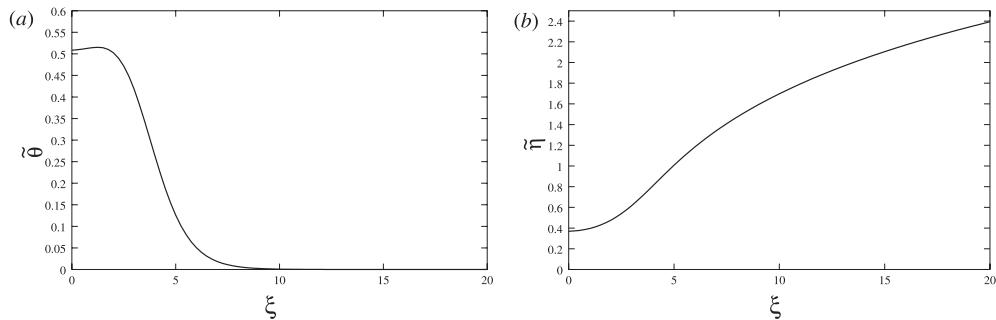

Figure 11. Sharp distributions (*a*) $\tilde{\theta}(\xi)$ and (*b*) $\tilde{\eta}(\xi)$ in a two-dimensional radially symmetric static AS, obtained from the numerical solution of equations (4.5) and (4.6) with $\tilde{A} = 5$.

$\tilde{A} \sim (\ln \epsilon^{-1})^{-1/2}$. It is easy to show that, similarly to the one- and three-dimensional cases, the solution in the form of the two-dimensional AS will disappear at $A < A_b \sim \epsilon(\ln \epsilon^{-1})^{1/2}$.

At $\tilde{A}$ sufficiently small, the AS looks like a spike with the maximum value of $\tilde{\theta}$ centred at $\xi = 0$. As in the case of the three-dimensional AS, when the value of A is increased, the AS gradually transforms into an annulus of radius R, which grows with $\tilde{A}$. According to equation (5.7), when R increases, we have $\bar{\theta} \sim R^{-1} \ll 1$ and $\bar{\eta} \sim \bar{\theta}$, so the potential $V_0 \sim \tilde{A}^2/R$ starts to dominate. An analysis similar to that for the three-dimensional AS shows that for $\tilde{A} \gg 1$ the parameters of the AS are given by

$$R^* = \tfrac{1}{6}\tilde{A}^2 \qquad \bar{\eta}_s^* = 1. \tag{5.12}$$

These results are also supported by the numerical solution of the equations for the sharp distributions. The dependences of $\tilde{\eta}(0)$ and $\tilde{\theta}(0)$ on $\tilde{A}$ are presented in figure 10. The solution of equations (4.5) and (4.6) in the form of the two-dimensional radially symmetric static spike AS at a particular value of $\tilde{A}$ is also presented in figure 11. Of course, when $R \sim \epsilon^{-1}$, the approximations made in the derivation of the equations for the sharp distributions are no longer valid, so, as in the case of the three-dimensional radially symmetric AS, the two-dimensional radially symmetric AS of radius R^* will transform into a quasi-one-dimensional AS of infinite radius. According to equation (5.12), this will happen when $A > A_d \sim \epsilon^{1/2} \ln \epsilon^{-1}$.

Finally, we note that the small parameter of the singular perturbation expansion in the two-dimensional case turned out to be $1/\ln \epsilon^{-1}$, so one should expect it to give a good quantitative agreement with the actual solutions only for extremely small values of ϵ. Nevertheless, the

leading scaling given by equation (5.4) (up to the logarithmic terms) should be in good agreement even for not very small ϵ. Also, it is not difficult to modify the theory in such a way that it uses ϵ as a small parameter in the expansion. In that case the sharp distributions will contain a weak logarithmic dependence on ϵ.

6. Discussion

While the work on this paper was being done, a number of publications on the Gray–Scott model appeared in the literature. The publications that are most relevant to our analysis are those of [45, 46]. Let us also mention a paper conceerning spike solutions in the Gray–Scott model on a finite domain [49].

In [46] Doelman *et al* present an asymptotic study of the static ASs and periodic strata in the one-dimensional Gray–Scott model. They perform a singular perturbation analysis of the localized and spatially periodic stationary solutions in a limited region of the parameter space. Doelman *et al* do not use the natural scaling of the Gray–Scott model given by equations (2.13) and (2.14). Instead, they introduce dimensionless quantities such that the original equations (2.3) and (2.4) become (we use the notation of [48])

$$\frac{\partial U}{\partial t} = \frac{\partial^2 U}{\partial x^2} - UV^2 + \delta^2 a(1 - U) \tag{6.1}$$

$$\frac{\partial V}{\partial t} = \delta^2 \frac{\partial^2 V}{\partial x^2} + UV^2 - \delta^\beta bV \tag{6.2}$$

where U is the inhibitor, V is the activator, δ is the small parameter, a and b are constants of the order of one, and β $(= 2\alpha/3$ from [46]) is a parameter that lies in the interval from zero to one. The solutions are studied in the limit $\delta \to 0$. It is easy to see that equations (6.1) and (6.2) can be reduced to equations (2.13) and (2.14) with

$$\epsilon = \delta^{(4-\beta)/2} \sqrt{\frac{a}{b}} \qquad \alpha = \delta^{2-\beta} \frac{a}{b} \qquad A = \delta^{1-\beta} \frac{\sqrt{a}}{b}. \tag{6.3}$$

Observe that the scaling in equations (6.1) and (6.2) forces certain relations between the parameters ϵ, α and A, so, in fact, such a choice of scaling significantly restricts the parameter space studied by Doelman *et al*.

According to the results of [46], the static one-dimensional AS exists when $\beta \in [0, 1)$ as $\delta \to 0$. This statement is based on the fact that the coefficient in front of the last term on the right-hand side of equation (6.1) scales as δ^2. On the other hand, as we showed in section 3, this AS in fact exists over a wider range of the parameters as long as $\epsilon \ll 1$, so, in fact, such a scaling is not a necessary condition for the AS existence.

The case $\beta = 0$ is equivalent to $A \sim A_b$ in our notation. Our result that the solution exists only at $A > A_b = \sqrt{12\epsilon}$ is in agreement with the result of [46] that the solution exists at $a > 144b^3$. Note that the analogous method of finding A_b for the ASs in systems of small size was introduced two decades ago by Kerner and Osipov [16]. There they performed an analysis of a very similar model—the Brusselator. The results obtained by them at $A \sim A_b$ for the Brusselator differ from those presented in our paper only by numerical coefficients. A calculation similar to that of section 3.1 was performed by Dubitskii *et al* for the Gierer–Meinhardt model [36] (see also [11]). Osipov and Severtsev also performed such an analysis for a simplified version of the Gray–Scott model, which is also very similar to the results of the first part of section 3 [39]. The advantage of the method of Doelman *et al*, however, is that it rigorously shows the existence of the static spike AS for $A_b \lesssim A \ll 1$ and $\epsilon \ll 1$.

The case $0 < \beta < 1$ is equivalent to that considered by us in section 3.3. The leading-order approximation to the solution obtained by Doelman *et al* is in agreement with the one obtained in equation (3.22) of our paper. The case $\beta = 1$ is equivalent to our $A \sim 1$. In [48], Doelman *et al* used topological shooting to show that the solutions do not exist for $\delta^{1-\beta} \gg 1$. This is in agreement with the results of section 3.2 of our paper that the static spike ASs do not exist for $A \gg 1$. We, on the other hand, used the nonlinear eigenvalue problem to study the solutions at $A \sim 1$ and, furthermore, showed that the solution disappears at $A = A_d = 1.35$ in the limit $\epsilon \to 0$.

Reynolds, Ponce-Dawson and Pearson derived an asymptotic equation of motion for the spike AS in the Gray–Scott model with $A \sim 1$, $\alpha \sim 1$ and $\epsilon \ll 1$ (in our notation). The reason the AS moves is its interaction with the boundary. These equations also describe the static spike AS. For $A > A_d$ the peculiarities of the internal dynamics result in the breakdown of the asymptotic description which the authors attribute to splitting and self-replication of the AS. The equations obtained by the authors for the inner region, in fact, coincide with equations (3.12) and (3.13) obtained by us in section 3.2 in the case of the static spike AS. They also found the value of A_d which agrees with the one obtained by us.

Finally, we mention recent studies by Hale *et al* [50]. They found exact solutions in the form of solitary pulses and fronts, and analysed their stability in the Gray–Scott model with $\epsilon = 1$ and $\alpha = \epsilon^2$. For these ϵ and α one can introduce the new variables $\tilde{\theta} = \theta/A$ and $\tilde{\eta} = \eta + (\epsilon^2/A)\theta$ which turn out to be decoupled; so the dynamics of the system is described by a scalar reaction–diffusion equation [47]. It is then not surprising that the behaviour of the system remains the same if ϵ is close to, but not exactly equal to 1 [50].

7. Conclusion

In conclusion, we performed an asymptotic analysis of the static spike ASs—self-sustained localized inhomogeneous states—in the Gray–Scott model of an autocatalytic chemical reaction. We showed that the solutions in the form of the static autosolitons exist in certain parameter regions when the ratio ϵ of the characteristic length scales of the activator and the inhibitor is small. These solutions have the form of narrow spikes of the concentration of the activator substance.

In one dimension, the static spike ASs exist over a broad range $A_b < A < A_d$, with $A_b \sim \epsilon^{1/2}$ and $A_d \sim 1$, with large amplitude $\theta_{max} \sim A\epsilon^{-1}$ (section 3). When the value of A approaches A_b from above, the amplitude of the AS decreases and at $A = A_b$ the solution abruptly disappears. On the other hand, when the value of A approaches A_d from below, the distribution of the activator in the spike flattens, until at $A = A_d$ the AS splits into two with the consecutive self-replication of the newborn spots [45, 47]. Note that even for A close to $A_b \sim \epsilon^{1/2} \ll 1$, that is, in such a weakly non-equilibrium system, the AS can have a gigantic amplitude of the order of $\epsilon^{-1/2} \gg 1$.

In contrast to the one-dimensional case in which the static spike ASs exist over a wide range of the parameter A, in three dimensions the region of existence of the static radially symmetric spike AS is substantially narrower. Indeed, as we showed in section 4, the static three-dimensional radially symmetric AS exists when $A_b < A < A_d$, when now $A_b \sim \epsilon$ and $A_d \sim \epsilon^{1/2}$. The maximum value of the activator in the AS is also large: $\theta_{max} \sim \epsilon^{-1}$. As in the case of the one-dimensional AS, when the value of A is decreased, at $A = A_b$ the solution in the form of the static three-dimensional radially symmetric spike AS abruptly disappears. When the value of A is increased, the AS gradually transforms from the spike to an annulus. Note that the solution in the form of the annulus is always unstable with respect to the radially

nonsymmetric breakup [47], so the static radially symmetric ASs are realized only at $A \sim \epsilon$ in three dimensions. Similar conclusions can also be made concerning the static spike ASs in two dimensions. In this case $A_b \sim \epsilon(\log \epsilon^{-1})^{1/2}$ and $A_d \sim \epsilon^{1/2} \log \epsilon^{-1}$.

Acknowledgments

References

[1] Nicolis G and Prigogine I 1977 *Self-Organization in Nonequilibrium Systems* (New York: Wiley)
[2] Vasiliev V A, Romanovskii Y M, Chernavskii D S and Yakhno V G 1987 *Autowave Processes in Kinetic Systems* (Berlin: VEB)
[3] Field R J and Burger M (ed) 1985 *Oscillations and Traveling Waves in Chemical Systems* (New York: Wiley)
[4] Murray J D 1989 *Mathematical Biology* (Berlin: Springer)
[5] Cross M C and Hohenberg P S 1993 *Rev. Mod. Phys.* **65** 851
[6] Mikhailov A S 1990 *Foundations of Synergetics* (Berlin: Springer)
[7] Kapral R and Showalter K 1995 *Chemical Waves and Patterns* (Dordrecht: Kluwer)
[8] Kerner B S and Osipov V V 1986 *Nonlinear Irreversible Processes* ed W Ebeling and H Ulbricht (Berlin: Springer)
[9] Kerner B S and Osipov V V 1989 *Sov. Phys.–Usp.* **32** 101
[10] Kerner B S and Osipov V V 1990 *Sov. Phys.–Usp.* **33** 3
[11] Kerner B S and Osipov V V 1994 *Autosolitons: a New Approach to Problem of Self-Organization and Turbulence* (Dordrecht: Kluwer)
[12] Niedernostheide F J (ed) 1994 *Nonlinear Dynamics and Pattern Formation in Semiconductors and Devices* (Berlin: Springer)
[13] Bode M and Purwins H-G 1995 *Physica* D **86** 53
[14] Gorman M, El Hamdi M and Robbins K A 1994 *Combust. Sci. Technol.* **98** 37
  Gorman M, El Hamdi M and Robbins K A 1994 *Combust. Sci. Technol.* **98** 71
  Gorman M, El Hamdi M and Robbins K A 1994 *Combust. Sci. Technol.* **98** 79
[15] Lee K J, McCormick W D, Ouyong Q and Swinney H L 1993 *Science* **261** 192
  Lee K J, McCormick W D, Pearson J E and Swinney H L 1994 *Nature* **369** 215
  Lee K J and Swinney H L 1995 *Phys. Rev.* E **51** 1899
[16] Kerner B S and Osipov V V 1978 *Sov. Phys.–JETP* **47** 874
  Kerner B S and Osipov V V 1982 *Biophys. (USSR)* **27** 138
  Kerner B S and Osipov V V 1985 *Sov. Phys.–JETP Lett.* **41** 473
[17] Kerner B S and Osipov V V 1979 *Sov. Phys.–Semicond.* **13** 424
  Kerner B S and Osipov V V 1979 *Sov. Phys.–Solid State* **21** 1348
[18] Kerner B S and Osipov V V 1980 *Sov. Phys.–JETP* **52** 1122
  Kerner B S and Osipov V V 1981 *Sov. Microelectronics* **10** 407
[19] Koga S and Kuramoto Y 1980 *Prog. Theor. Phys.* **63** 106
[20] Petrich D M and Goldstein R E 1994 *Phys. Rev. Lett.* **72** 1120
  Goldstein R E, Muraki D J and Petrich D M 1996 *Phys. Rev.* E **53** 3933
[21] Muratov C B and Osipov V V 1996 *Phys. Rev.* E **53** 3101
[22] Muratov C B and Osipov V V 1996 *Phys. Rev.* E **54** 4860
[23] Hagberg A and Meron E 1994 *Phys. Rev. Lett.* **72** 2492
  Hagberg A and Meron E 1994 *Chaos* **4** 477
  Elphick C, Hagberg A and Meron E 1995 *Phys. Rev.* E **51** 3052
[24] Muratov C B 1997 Theory of domain patterns in systems with long-range interactions of Coulombic type *PhD Thesis* Boston University
[25] Kerner B S and Osipov V V 1985 *Sov. Phys.–JETP* **62** 337
[26] Pearson J E 1993 *Science* **261** 189
[27] Ortoleva P J and Ross J 1975 *J. Chem. Phys.* **63** 3398
  Casten R G, Cohen H and Lagerstrom A 1975 *Q. Appl. Math.* **32** 365
[28] Kerner B S and Osipov V V 1982 *Sov. Phys.–JETP* **56** 1275
  Gafiichuk V V, Kerner B S, Lazurchak I M and Osipov V V 1986 *Mikroelektronika* **15** 180

Osipov V V, Gafiichuk V V, Kerner B S and Lazurchak I M 1987 *Mikroelektronika* **16** 23
Gafiichuk V V, Gashpar V E, Kerner B S and Osipov V V 1988 *Sov. Phys.–Semicond.* **22** 1298
[29] Kerner B S and Osipov V V 1983 *Mikroelektronika* **12** 512
Dockery J D and Keener J P 1989 *SIAM J. Appl. Math.* **49** 539
[30] Kuznetsova E M and Osipov V V 1995 *Phys. Rev. E* **51** 148
[31] Krischer K and Mikhailov A 1994 *Phys. Rev. Lett.* **73** 3165
[32] Schutz P, Bode M and Gafiichuk V V 1995 *Phys. Rev. E* **52** 4465
[33] Osipov V V 1996 *Physica D* **93** 143
[34] Gierer A and Meinhardt H 1972 *Kybernetik* **12** 30
[35] Gray P and Scott S 1983 *Chem. Eng. Sci.* **38** 29
[36] Dubitskii A L, Kerner B S and Osipov V V 1989 *Sov. Phys.–Dokl.* **34** 906
[37] Osipov V V 1993 *Phys. Rev. E* **48** 88
[38] Osipov V V and Muratov C B 1995 *Phys. Rev. Lett.* **75** 388
[39] Osipov V V and Severtsev A V 1996 *Phys. Lett.* A **222** 400
Osipov V V and Severtsev A V 1997 *Phys. Lett.* A **227** 61
[40] Osipov V V and Severtsev A V 1998 *Physica A* **249** 162
[41] Katz B 1966 *Nerve, Muscle and Synapse* (New York: McGraw-Hill)
[42] Wood P M and Ross J 1985 *J. Chem. Phys.* **82** 1924
[43] Vinoslavskii M N 1989 *Sov. Phys.–Solid State* **31** 1461
Vinoslavskii M N, Kerner B S, Osipov V V and Sarbej O G 1990 *J. Phys.–Cond. Mat.* **2** 2863
[44] Purwins H-G *et al* 1989 *Phys. Lett.* A **136** 480
Willebrandt H *et al* 1990 *Phys. Lett.* A **149** 131
[45] Reynolds W N, Pearson J E and Ponce-Dawson S 1994 *Phys. Rev. Lett.* **72** 2797
Reynolds W N, Pearson J E and Ponce-Dawson S 1997 *Phys. Rev. E* **56** 185
[46] Doelman A, Kaper T J and Zegeling P 1997 *Nonlinearity* **10** 523
[47] Muratov C B and Osipov V V 2000 Spike autosolitons in the Gray–Scott model *CAMS Report* 9900–10, NJIT,
    Newark, NJ 07102 (available at LANL archive: patt-sol/9804001)
[48] Doelman A, Gardner R A and Kaper T J 1998 *Physica D* **122** 1
[49] Wei J 1999 *Nonlinearity* **12** 593
[50] Hale J K, Peletier L A and Troy W C 2000 *SIAM J. Appl. Math.* **61** 102